# Alpha Heating of Indirect drive Layered Implosions on the National Ignition Facility

K. L. Baker[1], S. MacLaren[1], O. Jones[1], B. K. Spears[1], P. K. Patel[1], R. Nora[1], L. Divol[1], O. L. Landen[1], G. J. Anderson[1], J. Gaffney[1], M. Kruse[1], O. A. Hurricane[1], D. A. Callahan[1], A. R. Christopherson[1], J. Salmonson[1], E. P. Hartouni[1], T. Döppner[1], E. Dewald[1], R. Tommasini[1], C. A. Thomas[2], C. Weber[1], D. Clark[1], D. T. Casey[1], M. Hohenberger[1], S. Khan[1], T. Woods[1], J. L. Milovich[1], R. L. Berger[1], D. Strozzi[1], A. Kritcher[1], B. Bachmann[1], R. Benedetti[1], R. Bionta[1], P.M. Celliers[1], D. Fittinghoff[1], R. Hatarik[1], N. Izumi[1], M. Gatu Johnson[3], G. Kyrala[4], T. Ma[1], K. Meaney[4], M. Millot[1], S. R. Nagel[1], A. Pak[1], P. L. Volegov[4], C. Yeamans[1], C. Wilde[4]

1 Lawrence Livermore National Laboratory

2 Laboratory for Laser Energetics, University of Rochester

3 Massachusetts Institute of Technology

4 Los Alamos National Laboratory

**Abstract**

In order to understand how close current layered implosions in indirect-drive inertial confinement fusion (ICF) are to ignition, it is necessary to measure the level of alpha heating present. To this end, pairs of experiments were performed which consisted of a low yield "tritium-hydrogen-deuterium (THD)" layered implosion and a high yield "deuterium-tritium (DT)" layered implosion to experimentally validate current simulation-based methods of determining yield amplification. The THD capsules were designed to simultaneously reduce DT neutron yield(alpha heating) and maintain hydrodynamic similarity with the higher yield DT capsules. The ratio of the yields measured in these experiments then allowed the alpha heating level of the DT layered implosions to be determined. The level of alpha heating inferred is consistent with fits to

simulations expressed in terms of experimentally measurable quantities and enables us to infer the level of alpha heating in recent high performing implosions.

In an inertially-confined fusion (ICF) implosion with a deuterium-tritium (DT) fuel layer, each fusion reaction of deuterium and tritium ions generates a 14.1 MeV neutron and 3.5 MeV alpha-particle.[1] The areal density (ρR) required to stop the fusion neutron (> 5 g/cm$^2$) is generally far above what is present in an ICF implosion.[1] As such, the majority of neutrons leave the implosion without interacting with the hotspot or the ice layer surrounding the hotspot. The stopping ρR for an alpha-particle, however, is only ~0.1-0.2 g/cm$^2$ at an ion temperature, $T_{ion}$, of 4 keV, which is characteristic of the hot-spot ρR and $T_{ion}$ conditions achieved in many ICF implosions on the National Ignition Facility (NIF). Each of the alpha-particles stopped within the hot-spot deposit their 3.5 MeV of energy increasing the hotspot ion temperature, $T_{ion}$, and subsequently the reactivity-rate. The ρR required to stop alpha-particles increases with electron temperature(alpha-electron collisions are primarily responsible for stopping) such that alpha's not stopped in the hot-spot are stopped in the cold DT fuel surrounding the hot-spot where ρR values are ~0.4 to 1 g/cm$^2$. The alpha-particles stopped in the cold fuel heat and ablate the fuel into the hot-spot, increasing the hotspot mass ($M_{hs}$) and the hot-spot ρR, enabling more of the subsequent alpha-particles to be stopped within the hot-spot. An ignited plasma is one where the fusion heating power is high enough to overcome all of the physical processes that cool the fusion plasma. This creates a positive thermodynamic feedback loop with rapidly increasing temperature.

The radiation hydrodynamics code Hydra was used to perform a series of hydroscaled simulations covering a range of yield amplifications, $Y_{amp}$, from ~1 to greater than 40.[2] The capsule-only simulations perfectly hydroscaled the implosion at the time of peak kinetic energy, the start of the deceleration phase. The radiation temperature drive was linearly scaled in time by the scale factor S and the capsule dimensions were scaled by the scale factor S. This produced the

same adiabat, implosion velocity etc. between the hydroscaled implosions. As the scale is increased, ρR also increases which increases the self-heating and the yield amplification. These simulations were based on the BigFoot platform as were the experiments described below because at the time it had achieved the highest $Y_{amp}$ levels on the NIF. [3-8] This level of performance has been surpassed in recent high yield shots but the Bigfoot data set allows validation of the technique described below. Determining the degree that alpha-heating contributes to the yield is straightforward in simulations as alpha heating can be turned off. The $Y_{amp}$ from these simulations can be fit by simulation parameters whose experimental counterparts can be directly measured and fits based on these simulations, for the ignition threshold factor, ITFXmod, and the yield amplification, $Y_{amp\text{-}ITFXmod}$, are given in equations 1 and 2.

$$ITFXmod \sim (19.7*DSR)^2*(0.24*(4f_Df_T)*Y_{13\text{-}15}/(M_{fuel})) \quad \text{and} \quad (1$$

$$Y_{amp\text{-}ITFXmod} \sim \exp(ITFXmod^{0.446}), \quad (2$$

where DSR is the down scattered ratio (the ratio of the neutron yield in the neutron kinetic energy range from 10 - 12 MeV to the 13 - 15 MeV range), $f_D$ is the deuterium number fraction in the hotspot, $f_T$ is the tritium number fraction in the hotspot, $Y_{13\text{-}15}$ is the primary neutron yield/$10^{16}$ and $M_{fuel}$ is the initial mass of the ice layer in mg. These fits are very similar to the equations determined for the $Y_{amp}$ in direct drive implosions [9] and in indirect drive implosions [10]. The modified yield amplification fit in eqs. 1 and 2, $Y_{amp\text{-}ITFXmod} \sim \exp(7.56*DSR^{0.9}((4f_Df_T)Y_{13\text{-}15}/M_{fuel})^{0.45})$, differs slightly from the conventional yield amplification, $Y_{amp\text{-}ITFX} \sim \exp(8.67*DSR^{0.99}(Y_{13\text{-}15}/M_{fuel})^{0.47})$ [10], calculated from the ignition threshold factor, ITFX. The simulated $Y_{amp}$ as a function of capsule absorbed energy, red circles, and $ITFXmod^{1.3}$, black circles, are shown in Figure 1a along with the dashed line fits calculated from equation 1 and 2 (red and black) and the conventional ITFX(blue) using simulated observables. These simulations

added preheat energy to the DT ice, 0.75 MJ/g, a few hundred picoseconds before the time of peak implosion velocity which enabled them to match the experimental observables for this platform. This added ~ 70 J to a 45 um thick DT ice layer and changed the adiabat from the design of 4.0 to approximately 5.9. A separate set of Hydra simulations encompassing the experiments performed in this campaign were conducted to also test the scaling of eq. 1 and 2 on THD implosions where the fraction of deuterium ions in the ice layer was less than 50%. These simulation results are shown in Fig. 1b where the simulated $Y_{amp}$ for each implosion is represented on the x-axis and the fit using eq. 1 and 2 with simulated DSR, primary yield and ice mass is represented on the y-axis. These simulations led to the incorporation of the term $4f_Tf_D$ in eq. 1. With this term included(red circles), eq. 1 and 2 provided good fits to both the DT and THD simulated $Y_{amp}$. When this term was removed from eq. 1(green circles), the fit overestimated the $Y_{amp}$ for THD implosions with $f_D<0.5$.

The level of alpha-heating in DT layered implosions can be determined by comparing the yield of a hydrodynamically similar implosion with diluted fuel to that of a 50/50 DT layered implosion. The diluted fuel consists of specific ratios of tritium, hydrogen and deuterium ions (THD) to conserve the layer mass, usually with the deuterium fraction being very small, around 5%, to limit the yield and the $Y_{amp}$.[11,12] Specifically, the fraction of hydrogen atoms, $n_H$, and tritium atoms, $n_T$, in terms of the number of deuterium atoms, $n_D$, is given by $n_H = 0.25\text{-}0.5*n_D$ and $n_T = 0.75\text{-}0.5*n_D$.[11,12] The $Y_{amp}$ of the DT experiment can then be determined from the relationship:

$$Yamp \equiv \frac{Y_{DT}}{Y_{DT\alpha-off}} = \frac{Y_{DT}}{Y_{THD}} \frac{Y_{THD}}{Y_{THD\alpha-off}} \frac{Y_{THD\alpha-off}}{Y_{DT\alpha-off}} \quad (3$$

where $Y_{DT}$ and $Y_{THD}$ are the yields measured in the separate DT and THD fuel experiments using nominally identical targets and laser drives, and $Y_{DT\alpha\text{-off}}$ is the DT yield if alpha-particles didn't deposit their energy in the hotspot or ice layer. The ratio $Y_{THD}/Y_{THDa\text{-off}}$ is slightly above 1, 1.04 to 1.14, due to a reduced, but non-zero, alpha-heating contribution to its yield for the THD implosions described herein. This is estimated from simulations or equations 1 and 2 above and varies primarily due to the fuel composition in the THD implosion. The ratio of $Y_{THD\alpha\text{-off}}/Y_{DT\alpha\text{-off}}$ is given by the ratios of products of reactant fractions multiplied by factors correcting for hydrodynamic similarity deviations`

$$\frac{Y_{THD\alpha-off}}{Y_{DT\alpha-off}} \approx \frac{f_{D_{THD}} f_{T_{THD}}}{f_{D_{DT}} f_{T_{DT}}} \frac{1}{\beta} \left( \frac{1-\left(v_{hs_THD}/v_{imp_THD}\right)^2}{1-\left(v_{hs_DT}/v_{imp_DT}\right)^2} \right)^{3.6} \left( \frac{v_{imp_THD}}{v_{imp_DT}} \right)^{6.2}. \quad (4$$

A value of $\beta \sim 1.3$ represents the average value of $\beta$ vs. ITFX for a range of simulations required to correct $Y_{THD\alpha\text{-off}}/Y_{DT\alpha\text{-off}}$ for deviations from hydrodynamic similarity between the THD and no-alpha heating DT layered implosions due to adiabat(compression) and THD concentrations at the place of peak weighted neutron burn as seen in Fig. 6a in reference [13]. For this article we also corrected the 1D yield for the differences in the residual mode 1 hotspot velocity observed between the DT and THD implosions using the analytic expression,$Y \alpha (1-(v_{hs}/v_{imp})^2)^{3.6}$, where $v_{hs}$ is the velocity of the hotspot and $v_{imp}$ is the peak implosion velocity of the capsule.[14-16] This led to corrections in $Y_{amp}$ of up to $\pm$16%. The yield is also corrected for differences in the implosion velocities of the DT and THD implosions, using the analytic expression $Y \alpha v_{imp}^{6.2}$.[14] The difference in implosion velocity between the DT and THD pairs, however, were all less than ~2% which is less than the absolute precision of the velocity from the simulation, $\pm$3.5%.

These experiments were conducted using the BigFoot platform and they were carried out with two different hohlraum and capsule sizes. [3-8] The experiments used high-density carbon

(HDC) capsules with an inner-capsule radius of 950(844) μm for the larger scale(smaller scale). and the capsule thickness was 72(68.3) μm for the larger scale(smaller scale). The capsule walls were comprised of three layers: an outer, ~44.5(40.4) μm thick pure HDC layer, followed by a ~21.4(21.9) μm thick, tungsten-doped layer with average dopant levels of 0.24%(0.32%) atomic fraction, and an innermost, undoped HDC layer of 6.3(6) μm for the larger scale(smaller scale). The fusion fuel added to the inside of the capsules, THD or DT, had a layer thickness of ~45(40) μm for the larger scale(smaller scale). These capsules were placed in the center of a gold hohlraum of 11.3 (10.13) mm length and 6.0 (5.4) mm diameter with laser entrance holes (LEHs) at either end of the hohlraum with a diameter of 3.9 (3.45) mm, for the larger scale (smaller scale). The hohlraums in both cases were filled with low-density 4He gas at 0.3 mg/cm$^3$ to tamp the expansion of hohlraum wall and ablator material, provide heat conduction to the hohlraum walls and minimize the laser-plasma instabilities inside the hohlraum. The pulse shapes used for the larger (black) and smaller (red) scale experiments are shown in Figure 2. Both the DT layered implosion and the THD layered implosion performed at each scale used the same laser pulse shape.

When determining the $Y_{amp}$ present in the experiments, the relative hotspot mass originating from the vapor and from the ice must be determined so as to calculate the effective hotspot concentrations used in Eq. 1 and 3. The hotspot mass, $M_{hs}$, can be expressed as $M_{hs}= \rho V_{hs}$ and was calculated from the experimental measurables using the methods in [18] and assuming the hotspot radius was 1.28x the 17% contour of the neutron image. This choice of the hotspot radius enabled the simple homogeneous model to more closely agree with the hotspot mass inferred from 3-D reconstructions of the hotspot neutron image.

To estimate the H, D, and T fractions in the hot-spot, the initial ratios of hydrogen isotopes in the solid fuel layer and in the saturated vapor interior to that layer were calculated. The

composition of the majority of the solid ice is the same as the initial reservoir gas mixture used to fill the capsule. Following a layering time (~17 hours), the solid reaches an equilibrium with the six diatomic molecular hydrogen species, $H_2$, $D_2$, $T_2$, HD, HT and DT.[17] The composition of the saturated vapor in the initial central gas region is in solid/vapor equilibrium with the solid layer and is determined by this species equilibrium. In the 30 seconds prior to a NIF shot the capsule is rapidly cooled by 0.8 K, a mini-quench, which sets the vapor concentrations in the center of the ablator at shot time. The initial vapor mass concentrations calculated this way along with the ice concentrations are listed in the second column of table 1. Given the final hotspot mass and the initial vapor mass concentrations inside the fuel, the effective THD concentration in the hotspot were determined and are also listed in the second column of table 1 within the square brackets. Given these final hotspot concentrations, the $Y_{amp}$ can be calculated using eq. 3 and 4 and compared with the fits to simulations expressed in terms of experimentaly measurable quantities expressed in eq. 1 and 2. In the DT layered implosions with a ~50/50 deuterium/tritium reservoir, this also leads to a slightly higher deuterium concentration in the hotspot than the optimal 50/50.

One of the deviations from hydrodynamic similarity between the DT and THD experimental pairs, represented by the β term in eq. 4, can be seen in the neutron hot spot images in Fig. 3a.[19] The initial saturated vapor concentrations inside the ice layer for each of the implosions is shown in Table 1 column 2 in parentheses along with the ice composition. This vapor is hydrogen/deuterium rich relative to the ice layer due to the difference in vapor pressure of the deuterium, tritium and hydrogen.[20] This leads to a higher initial electron density for the vapor inside the ice layer for the THD implosions which have a majority of hydrogen in the vapor in comparison to deuterium for the DT implosions. This higher initial number of electrons in the THD implosions is correlated with the final hotspot radius as shown in Fig. 3b. In the THD

implosion simulations, the peak of the burn was located some 10's of μm away from the center due to the radial distribution of gas species which also resulted in a larger hot spot than the corresponding DT implosion. In future experiments, the initial electron density can be reduced in the THD layered implosions by performing a larger quench, up to 1.5 K, than the DT implosion,reducing the β term in eq. 4.

When the terms in eq. 3 and 4 are calculated, the experimental yield amplification can be determined as shown in Fig. 4. Figure 4a shows the primary yield from each of the DT and THD implosions as blue bars. To isolate the yield dependence on reactant concentrations, the green bars represent the yield of the THD divided by the right-handside of Eq. 4(without the M1 and $v_{imp}$ corrections or $Y_{THD}\beta f_{D_{DT}} f_{T_{DT}} / f_{D_{THD}} f_{T_{THD}}$ and the red bars represent the green bars divided by the small $Y_{amp}$ of the THD pair or $Y_{THD\alpha-off}\beta f_{D_{DT}} f_{T_{DT}} / f_{D_{THD}} f_{T_{THD}}$. The $Y_{amp}$, without M1 or $v_{imp}$ corrections, is then simply the ratio of the DT primary yield (blue bar) to the red bar or $Y_{DT\alpha} f_{D_{THD}} f_{T_{THD}} / \left(Y_{THD\alpha-off}\beta f_{D_{DT}} f_{T_{DT}}\right)$. Figure 4b represents the $Y_{amp}$ as determined from the measurements in the experiments, as given by eq. 3 and 4, as a function of the $Y_{amp}$ using the empirical fit of the DSR, the initial DT mass and the primary yield, as given by eq. 1 and 2. In Figure 4b, the blue circles include the equation 4 approximation without M1 or $v_{imp}$ corrections. The red circles also include the equation 4 approximation with M1 but without $v_{imp}$ corrections and the green circles include all of the corrections listed in equation 4. As can be observed in Figure 4b and in table 1, the $Y_{amp}$ determined from the DT/THD pairs is within 20% of the $Y_{amp}$ fit to simulations (Eq.1 and 2) that has previously been applied to DT shots on the NIF. Ensemble simulations were performed on the implosions and closely matched the experimental yield, within 7%, and $Y_{amp}$ inferred using equation 1 and 2, within 6% with the M1 correction. Both the

yield(column 5) and $Y_{amp}$(column 11) from the simulations are shown in table 1 within the square brackets.

The ignition threshold factor, ITFXmod, can also be used to formulate a generalized Lawson criteria, GLC, for ignition which includes alpha heating and uses only the directly measured quantities of DSR, primary neutron yield and the initial ice mass. The previously defined GLC = $(P_{stag}/420)(E_{hs}/30)^{0.5}$ can be used along with the database of NIF layered implosions to determine the power scaling of ITFXmod resulting in a linear relationship between the two GLC definitions.[21] The stagnation pressure, $P_{stag}$, and hotspot energy, $E_{hs}$, used in this GLC are defined in [21] in Eqs. 17 and 14. Figure 5 then shows that a definition of

$$GLC(ITFXmod) = 0.27(ITFXmod)^{0.6} \quad (5$$

provides a linear relationship between the two generalized Lawson criteria, GLC(ITFXmod) as defined by Eq. 5 and the previously defined $GLC(P_{stag}, E_{hs}) = (P_{stag}/420)(E_{hs}/30)^{0.5}$, both of which include alpha heating. Fig. 5 also has plotted the ITFXmod for each of the experiments as a function of the $GLC(P_{stag}, E_{hs})$) and the fit to ITFXmod, $ITFXmod = 9(GLC(P_{stag}, E_{hs}))^{1.66}$, implies a value of ITFXmod = 9 at the ignition threshold, $GLC(P_{stag}, E_{hs}) = 1$. At this value of ITFXmod the yield amplification exceeds a value of ~14.4. As seen in Fig. 5, the implosion N210808 exceeds the threshold for ignition, GLC = 1, as reported in [22].

A series of experiments using pairs of THD/DT layered-implosions was conducted on the NIF to measure the level of alpha heating present in these implosions to understand how close they were to the burning plasma regime, $Y_{amp} \geq 3.5$, and to ignition, $Y_{amp} \geq 15$. These experiments allowed us to measure the $Y_{amp}$ experimentally with small corrections from simulations. We were also able to compare these measurements with fits to hydroscaled simulations of the BigFoot platform and confirm that the $Y_{amp}$ for these implosions were within ~20 % using these two

methods. Over the $Y_{amp}$ range studied in this campaign, 1.7 to 2.9, we found good agreement between the experimentally inferred $Y_{amp}$ and fits to simulation databases based on experimental observables, primary yield, DSR and initial layer mass, thus using experiments and simulations to verify the consistency of the alpha-heating models used to estimate the $Y_{amp}$. Verification of equations 1 and 2 with experiments enables us to look at more recent higher performing implosions and verify the levels of alpha heating present in those experiments. The DT implosions on the NIF were also used to define a generalized Lawson criteria, which includes alpha heating, based on the ignition threshold factor, ITFXmod, as given by Eq. 5. The recent high performing shot N210808 with a DSR or 2.72%, an initial ice mass of 220 μg and a primary yield of $4.3x10^{17}$, is predicted by equations 1 and 2 to have a yield amplification for that implosion at $24.8\pm6.2$, and the generalized Lawson criteria defined in Eq. 5 indicates that this implosion was past the ignition threshold of GLC=1, as reported in [22].

## REFERENCES


1) S. Atzeni and J. Meyer-ter-Vehn, The Physics of Inertial Fusion (Oxford Science Press, Oxford, 2004).

2) M. M. Marinak, R. E. Tipton, O. L. Landen, T. J. Murphy, P. Amendt, S. W. Haan, S. P. Hatchett, C. J. Keane, R. McEachern, and R. Wallace, "Three-dimensional simulations of Nova high growth factor capsule implosion experiments," Physics of Plasmas **3**, 2070 (1996)

3) K. L. Baker, C. A. Thomas, D. T. Casey, M. Hohenberger, S. Khan, B. K. Spears, O. L. Landen, R. Nora, T. Woods, J. L. Milovich, R. L. Berger, D. Strozzi, D. Clark, O. A. Hurricane, D. A. Callahan, A. Kritcher, B. Bachmann, R. Benedetti, R. Bionta, P.M. Celliers, D. Fittinghoff, C. Goyon, R. Hatarik, N. Izumi, M. Gatu Johnson, G. Kyrala, T. Ma, K. Meaney, M. Millot, S. R. Nagel, A. Pak, P. K. Patel, D. Turnbull, P. L. Volegov, C. Yeamans, C. Wilde, "Hotspot Parameter Scaling with Velocity and Yield for High Adiabat Layered Implosions on the National Ignition Facility" Phys. Rev. E **102**, 023210.

4) K. L. Baker, C. A. Thomas, D. T. Casey, S. Khan, B. K. Spears, R. Nora, T. Woods, J. L. Milovich, R. L. Berger, D. Strozzi, D. Clark, M. Hohenberger, O. A. Hurricane, D. A. Callahan, O. L. Landen, B. Bachmann, R. Benedetti, R. Bionta, P.M. Celliers, D. Fittinghoff, C. Goyon, G. Grim, R. Hatarik, N. Izumi, M. Gatu Johnson, G. Kyrala, T. Ma, M. Millot, S. R. Nagel, A. Pak, P. K. Patel, D. Turnbull, P. L. Volegov, C. Yeamans, "High-Performance Indirect-Drive Cryogenic Implosions at High Adiabat on the National Ignition Facility," Phys. Rev. Lett. **121**, 135001 (2018).

5) D. T. Casey, C. A. Thomas, K. L. Baker, B. K. Spears, M. Hohenberger, S. F. Khan, R. C. Nora, C. R. Weber, D. T. Woods, O. A. Hurricane, D. A. Callahan, R. L. Berger, J. L. Milovich, P. K. Patel, T. Ma, A. Pak, L. R. Benedetti, M. Millot, C. Jarrott, O. L. Landen, R. M. Bionta, B. J. MacGowan, D. J. Strozzi, M. Stadermann, J. Biener, A. Nikroo, C. S. Goyon, N. Izumi, S. R. Nagel, B. Bachmann, P. L. Volegov, D. N. Fittinghoff, G. P. Grim, C. B. Yeamans, M. Gatu Johnson, J. A. Frenje, N. Rice, C. Kong, J. Crippen, J. Jaquez, K. Kangas, and C. Wild, "The high velocity, high adiabat, "Bigfoot" campaign and tests of indirect-drive implosion scaling," Physics of Plasmas **25**, 056308 (2018).

6) C. A. Thomas, E. M. Campbell, K. L. Baker, D. T. Casey, M. Hohenberger, A. L. Kritcher, B. K. Spears, S. Khan, R. Nora, D. T. Woods, J. L. Milovich, R. L. Berger, D. Strozzi, D. D. Ho, D. Clark, B. Bachmann, R. Benedetti, R. Bionta, P. M. Celliers, D. Fittinghoff, G. Grim, R. Hatarik, N. Izumi, G. Kyrala, T. Ma, M. Millot, S. R. Nagel, P. K. Patel, C. Yeamans, A. Nikroo, M. Tabak, M. Gatu Johnson, P. L. Volegov, and S. M. Finnegan, "Deficiencies in compression and yield in x-ray driven implosions," Phys. Plasmas **27**, 112705 (2020).

7) M. Hohenberger, D. T. Casey, C. A. Thomas, O. L. Landen, K. L. Baker, L. R. Benedetti, D. A. Callahan, O. A. Hurricane, N. Izumi, S. F. Khan, T. Ma, D. A. Mariscal, S. R. Nagel, A. Pak, and B. K. Spears, "Maintaining low-mode symmetry control with extended pulse-shapes for lower-adiabat Bigfoot implosions on the National Ignition Facility," to be submitted to Phys. Plasmas.

8) Richard Berger, Cliff A. Thomas, Kevin Baker, Daniel Casey, Clement Goyon, Jaebum Park, Nuno Lemos, Shahab Khan, Matthias Hohenberger, Jose Milovich, David Strozzi, Mikhail Belyaev, Thomas Chapman, and A. Bruce Langdon, "Stimulated Backscatter of Laser Light from BigFoot hohlraums on the National Ignition Facility," Phys. Plasmas **26**, 012709 (2019).

9) R. Betti, A. R. Christopherson, B. K. Spears, R. Nora, A. Bose, J. Howard, K. M. Woo, M. J. Edwards, and J. Sanz, "Alpha Heating and Burning Plasmas in Inertial Confinement Fusion," Phys. Rev. Lett. **114**, 255003 (2015).

10) Pravesh K. Patel, Paul T. Springer, Christopher Weber, Leonard Charlie Jarrott, Omar A.Hurricane, Benjamin Bachmann, Kevin Baker, Laura Berzak Hopkins, Debra Callahan, Daniel T. Casey, Charles Cerjan, Daniel S. Clark, Eduard Liviu Dewald, Laurent Divol, Tilo Doeppner, John Everett Field, David N. Fittinghoff, Jim A Gaffney, Verena Geppert-Kleinrath, Gary Grim, Edward Paul Hartouni, Robert Hatarik, Denise Hinkel, Matthias Hohenberger, Kelli Humbird, Nobuhiko Izumi, Ogden S. Jones, Shahab F Khan, A. L. Kritcher, Michael Karl Gerhard Kruse, Otto Landen, Sebastien Le Pape, Tammy Ma, Stephan A. MacLaren, Andrew MacPhee, Laurent Pierre Masse, Nathan Meezan, Jose L. Milovich, Ryan Nora, Arthur Pak, Jayson Luc Peterson, Joseph Ralph, Harry F Robey, Jay D. Salmonson, Vladimir Smalyuk, Brian K. Spears, Cliff A. Thomas, Petr Volegov, Alex Zylstra, M. John Edwards," Hotspot conditions achieved in Inertial Confinement Fusion Experiments on the National Ignition Facility," Physics of Plasmas **27**, 050901 (2020).

11) M. J. Edwards, J. D. Lindl, B. K. Spears, S. V. Weber, L. J. Atherton, D. L. Bleuel, D. K. Bradley, D. A. Callahan, C. J. Cerjan, D Clark, G. W. Collins, J. E. Fair, R. J. Fortner, S. H. Glenzer, S. W. Haan, B. A. Hammel, A. V. Hamza, S. P. Hatchett, N. Izumi, B. Jacoby, O. S. Jones, J. A. Koch, B. J. Kozioziemski, O. L. Landen, R. Lerche, B. J. MacGowan, A. J. MacKinnon, E. R. Mapoles, M. M. Marinak, M. Moran, E. I. Moses, D. H. Munro, D. H. Schneider, S. M. Sepke, D. A. Shaughnessy, P. T. Springer, R. Tommasini, L. Bernstein, W. Stoeffl, R. Betti, T. R. Boehly, T. C. Sangster, V. Yu. Glebov, P. W. McKenty, S. P. Regan, D. H.

Edgell, J. P. Knauer, C. Stoeckl, D. R. Harding, S. Batha, G. Grim, H. W. Herrmann, G. Kyrala, M. Wilke, D. C. Wilson, J. Frenje, R. Petrasso, K. Moreno, H. Huang, K. C. Chen, E. Giraldez, J. D. Kilkenny, M. Mauldin, N. Hein, M. Hoppe, A. Nikroo, and R. J. Leeper, "The experimental plan for cryogenic layered target implosions on the National Ignition Facility—The inertial confinement approach to fusion," Phys. Plasmas **18**, 051003 (2011).

12) B. K. Spears, S. Brandon, D. Clark, C. Cerjan, J. Edwards,O. Landen, J. Lindl, S. Haan, S. Hatchett, J. Salmonson, P. Springer, S.V.Weber, and D. Wilson, "Prediction of ignition implosion performance using measurements of low-deuterium surrogates," J. Phys.: Conf. Ser. **244** 022014 (2010).

13) John Lindl, Otto Landen, John Edwards, Ed Moses, and the NIC Team, "Review of the National Ignition Campaign 2009-2012," Physics of Plasmas 21, 020501 (2014).

14) O. A. Hurricane , D. T. Casey, O. Landen , A. L. Kritcher, R. Nora , P. K. Patel , J. A. Gaffney , K. D. Humbird, J. E. Field, M. K. G. Kruse, J. L. Peterson, and B. K. Spears, "An analytic asymmetric-piston model for theimpact of mode-1 shell asymmetry on ICF implosions," Phys. Plasmas **27**, 062704 (2020); https://doi.org/10.1063/5.0001335

15) D. T. Casey, B. MacGowan, J. D. Sater, A. Zylstra, A. L. Kritcher, M. Hohenberger, K. Baker, S. Le Pape, T. Doeppner, C. Weber, H. Huang, O. L. Landen, J. Milovich, J. Biener, S. Haan, S. Ross, H. Robey, M. Stadermann, A. Nikroo, D. A. Callahan, O. A. Hurricane, M. Bruhn, C. Kong, K. Sequoia, N. Rice, C. Wild, "Evidence of Three-dimensional Asymmetries Seeded by HDC-ablator Non-uniformity in Experiments at the National Ignition Facility**,"** Phys. Rev. Lett. **126**, 025002 (2021).

16) Jose Milovich, D. Casey, Brian MacGowan, Daniel Clark, Derek Mariscal, Tammy Ma, K. Baker, Richard Bionta, Kelly Hahn, Alastair Moore, Dave Schlossberg, Ed Hartouni, Scott

Sepke, Otto Landen, "Understanding asymmetries using integrated simulations of capsule implosions in low gas-fill hohlraums at the National Ignition Facility," Plasma Phys. Control. Fusion **63**, 025012 (2021).

17) Brian K. Spears, "Cryogenic Fuel Composition for Layered Inertial Confinement Fusion Targets" Private Communication.

18) O. A. Hurricane, D. A. Callahan, D. T. Casey, P. M. Celliers, C. Cerjan, E. L. Dewald, T. R. Dittrich, T. Döppner , D. E. Hinkel, L. F. Berzak Hopkins, J. L. Kline, S. Le Pape, T. Ma, A. G. MacPhee, J. L. Milovich, A. Pak, H.-S. Park, P. K. Patel, B. A. Remington, J. D. Salmonson, P. T. Springer & R. Tommasini, "Fuel gain exceeding unity in an inertially confined fusion implosion," Nature **506**, 343 (2014).

19) Mark D. Wilke, Steven H. Batha, Paul A. Bradley, Robert D. Day, David D. Clark, Valerie E. Fatherley, Joshua P. Finch, Robert A. Gallegos, Felix P. Garcia, Gary P. Grim, Steven A. Jaramillo, Andrew J. Montoya, Michael J. Moran, George L. Morgan, John A. Oertel, Thomas A. Ortiz, Jeremy R. Payton, Peter Pazuchanics, Derek W. Schmidt, Adelaida C. Valdez, Carl H. Wilde, and Doug C. Wilson, " The National Ignition Facility Neutron Imaging System," Review of Scientific Instruments **79**, 10E529 (2008).

20) P. C. Souers, Hydrogen Properties for Fusion EnergyUniversity of California, Berkeley, 1986.

21) J. D. Lindl, S. W. Haan, O. L. Landen, A. R. Christopherson, and R. Betti, "Progress toward a self-consistent set of 1D ignition capsule metrics in ICF," Phys. Plasmas **25**, 122704 (2018); https://doi.org/10.1063/1.5049595

22) H. Abu-Shawareb, R. Acree, P. Adams et al., “Lawson Criterion for Ignition Exceeded in an Inertial Fusion Experiment,” Phys. Rev. Lett. **129**, 075001 (2022).

# FIGURE CAPTIONS

Figure 1a Simulated $Y_{amp}$ as a function of the capsule absorbed energy(red circles) and the modified ignition threshold factor(black circles), ITFXmod The fits to simulations expressed in terms of experimentaly measurable quantities, eq. 1 and 2, along with the simulated DSR, primary yield and ice mass are plotted as the dashed black and red lines and an fit using the conventional $Y_{amp\text{-}ITFX}$ is plotted as a dashed blue line in Fig. 1a. Fig. 1b motivates the includion of the factor $4f_Df_T$ in eq. 1. In a DT implosion this factor reduces to 1 but for THD implosions this factor was introduced to enable eq. 1 and 2 to provide an improved fit(red circles) vs. not including $4f_Df_T$ in eq. 1(green circles) for those cases where the deuterium fraction was less than 0.5. Figure 1b also shows the conventional $Y_{amp\text{-}ITFX}$, also with an inclusion of $4f_Df_T$, as yellow circles.

Figure 2 Laser power as a function of time for the larger scale N190707 layered implosion, solid black line, and for the smaller scale N190721 implosion, solid red line. The insert shows a schematic of the alpha heating process in which alpha heating of the plasma increases the temperature and reaction rate of the fusion process.

Figure 3 This figure shows the primary neutron images for the six implosions used in the alpha heating campaign in Figure 3a. The smaller scale DT-THD pairs of neutron images are shown in the top of the figure with the two DTs on the left-hand side; The larger scale DT-THD pairs of neutron images are shown on the bottom of the figure with the two DTs again on the left-hand side. Figure 3b show the initial electron density inside the ablator as a function of the final hotspot radius, P0

Figure 4 a) Shows the primary yield and $Y_{amp}$ from each of the DT and THD implosions. The blue bar represents the primary yield, the green bar represents the yield of the THD divided by eq.

4(without M1 and $E_L$ corrections) and the red bar represents the green bar divided by the calculated $Y_{amp}$ of the THD. Figure 4b represents the $Y_{amp}$ as determined from the measurements in the experiments, as given by eq. 3 and 4, as a function of the $Y_{amp}$ using the down-scattered ratio, the initial DT mass and the primary yield, as given by eq. 1 and 2. Blue circles represent no M1 or laser power $P_L$, corrections, red circles represent an M1 correction between the THD implosion and the no-alpha DT implosion and the green circles represent both an M1 and a $P_L$ correction between the THD implosion and the no-alpha DT implosion.

Figure 5 Linearity of the generalized Lawson criterion using the GLC(ITFXmod) = $0.27(\text{ITFXmod})^{0.6}$ defined in Eq. 2 plotted against the $\text{GLC}(P_{stag}, E_{hs}) = (P_{stag}/420)(E_{hs}/30)^{0.5}$. Both GLCs are calculated using the neutron metircs from the existing database of experimental DT layered implosions on the NIF. Also plotted is the ITFXmod as defined in Eq. 1.

Table 1 Summary of the two pairs of DT/THD experiments for which the $Y_{amp}$ has been determined experimentally.

# FIGURES

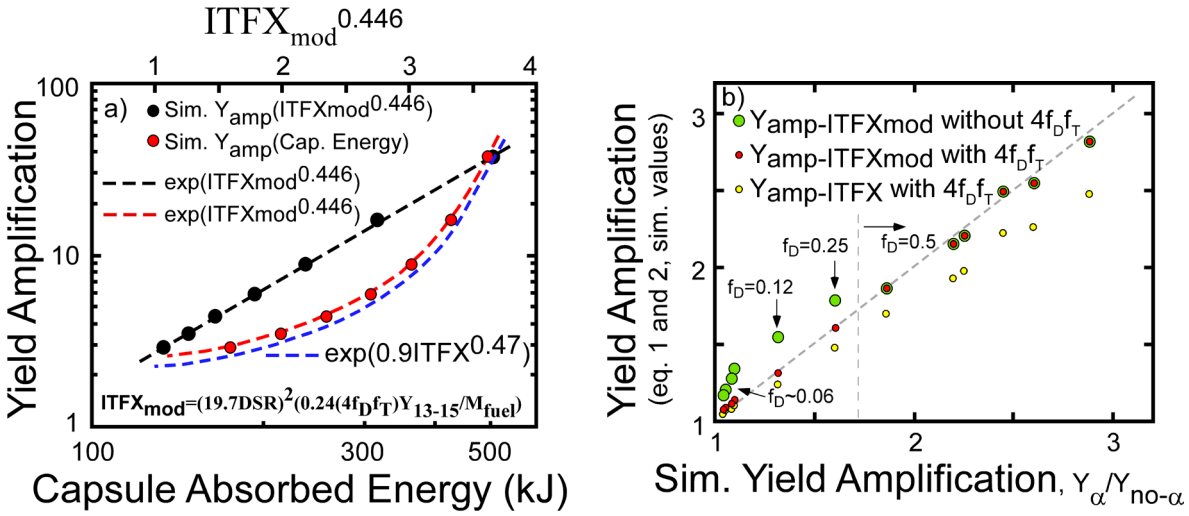


Figure 1

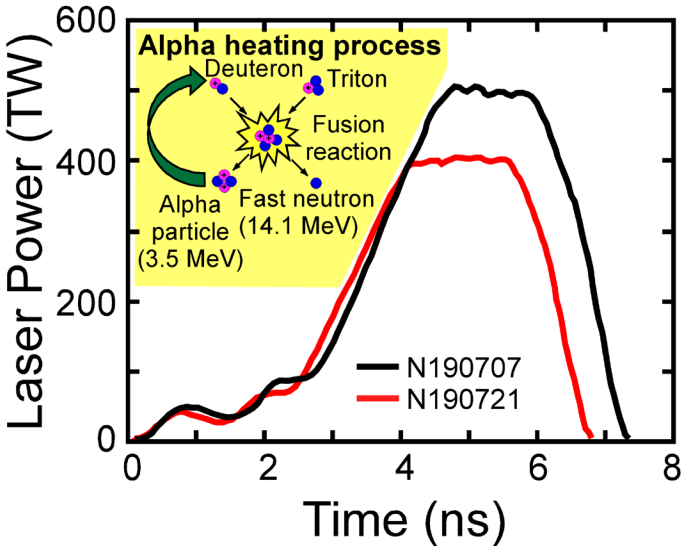
Alpha heating process
Deuteron
Triton
Fusion
reaction
Alpha
particle
(3.5 MeV)
Fast neutron
(14.1 MeV)
N190707
N190721
Laser Power (TW)
Time (ns)
0
200
400
600
0
2
4
6
8

Figure 2

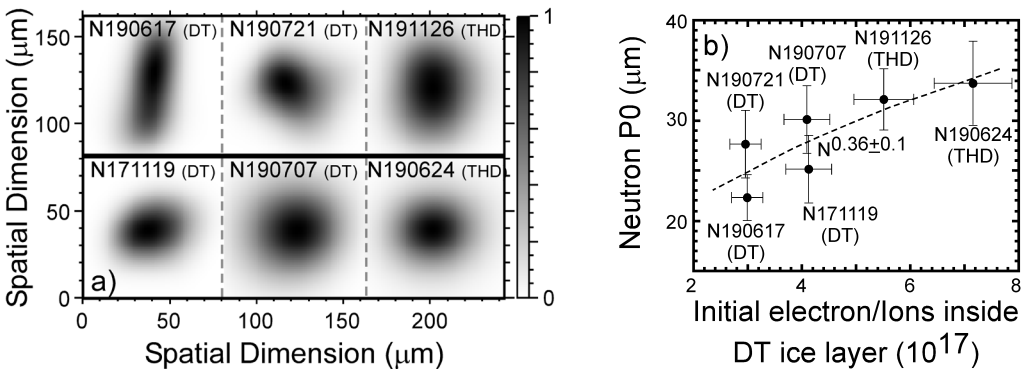
N190617 (DT)
N190721 (DT)
N191126 (THD)
N171119 (DT)
N190707 (DT)
N190624 (THD)
a)
Spatial Dimension (μm)
Spatial Dimension (μm)
1
0
b)
N190707 (DT)
N191126 (THD)
N190721 (DT)
N0.36±0.1
N190624 (THD)
N171119 (DT)
N190617 (DT)
Neutron P0 (μm)
Initial electron/Ions inside DT ice layer (10^17)

Figure 3

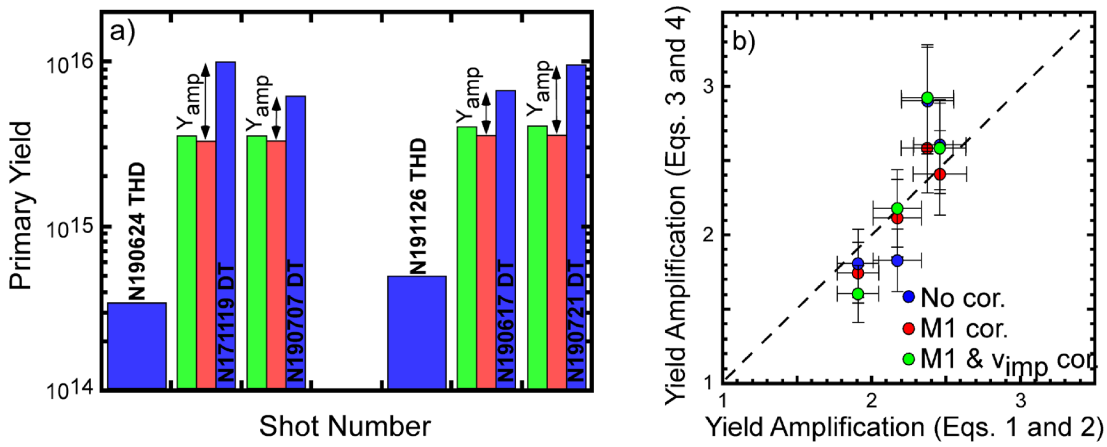
a)
Primary Yield
$10^{16}$
$10^{15}$
$10^{14}$
N190624 THD
$Y_{amp}$
N171119 DT
$Y_{amp}$
N190707 DT
N191126 THD
$Y_{amp}$
N190617 DT
$Y_{amp}$
N190721 DT
Shot Number
b)
Yield Amplification (Eqs. 3 and 4)
Yield Amplification (Eqs. 1 and 2)
1
2
3
No cor.
M1 cor.
M1 & $v_{imp}$ cor.

Figure 4

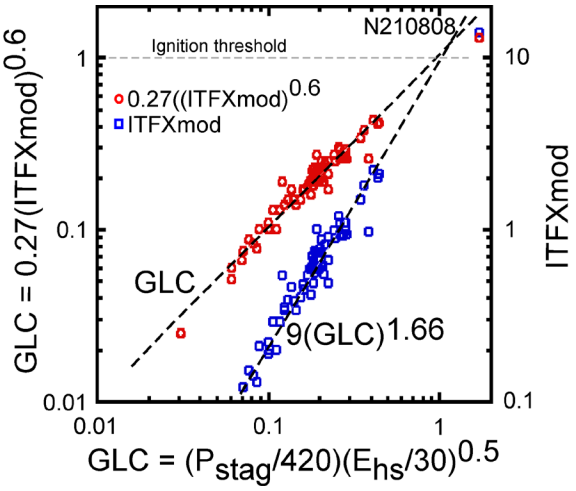
N210808
Ignition threshold
0.27((ITFXmod)^0.6
ITFXmod
GLC
9(GLC)^1.66
GLC = 0.27(ITFXmod)^0.6
ITFXmod
GLC = (P_stag/420)(E_hs/30)^0.5
1
0.1
0.01
10
1
0.1
0.01
0.1
1
Figure 5

Tables

| Shot # | Ice (Gas) [Hotspot] Composition THD (%) | Mhs (μg) [$f_T/f_D$] | Mvap (μg) [frac] | Total Yield ($10^{14}$) [sim] | Vhs/ Vimp | Vimp (km/sec) | $Y_{THD}$ YDTa-off | $Y_{THD}$ DTα–off Corr. | $Y_{amp}$ Eq. 3&4 M1 corr | $Y_{amp}$ Eq. 1&2 [sim] |
|---|---|---|---|---|---|---|---|---|---|---|
| N171119 DT 6x11.3 | 49.63:0.19:50.18 (33.85:0.67:61.6) [46.4:0.29:52.5] | 7.7 [0.88] | 1.56 [0.2] | 112 [114] | 0.12 | 411 | 0.126 | 0.089 | 2.6 | 2.4 [2.25] |
| N190707 DT 6x11.3 | 49.09/0.18/50.72 (32.75:0.66:61.3) [46.3:0.26:52.6] | 8.9 [0.88] | 1.56 [0.17] | 69.1 [73.4] | 0.20 | 426 | 0.126 | 0.113 | 1.7 | 1.9 [1.86] |
| N190624 THD 6x11.3 | 71.22/23.06/5.72 (18.9:73.3:3.1) [59.6:34.2:5.14] | 7.35 [11.3] | 1.63 [0.22] | 3.86 [3.62] | 0.22 | 420 | N/A | N/A | | 1.1 [1.05] |
| N190617 DT 5.4x10.13 | 49.41/0.18/50.41 (32.8:0.65:60.85) [46.7:0.26:52.1] | 6.8 [0.90] | 1.1 [0.16] | 74.5 [76.8] | 0.28 | 432 | 0.157 | 0.173 | 2.1 | 2.2 [2.2] |
| N190721 DT 5.4x10.13 | 50.48/0.18/49.34 (34.4:0.65:60.4) [48.7:0.23:50.5] | *9.87* [0.96] | 1.1 [0.12] | 107 [112] | 0.13 | 428 | 0.155 | 0.119 | 2.4 | 2.5 [2.6] |
| N191126 THD 5.4x10.13 | 71.47:21.87:6.67 (15.6:81.3:3.1) [62.6:31.3:6.1] | *7.85* [10.27] | 1.24 [0.15] | 5.38 [5.38] | 0.20 | 433 | N/A | N/A | | 1.14 [1.09] |

Table 1